

Effect of Molecular Weights of Poly(acrylic acid) on Crystallization of Calcium Carbonate by the Delayed Addition Method

By Shu-Chen HUANG, Kensuke NAKA,* and Yoshiki CHUJO[†]

The effect of poly(acrylic acid) (PAA) on the mineralization of CaCO_3 was studied by varying the molecular weights (PAA1.2k, $M_w = 1200$; PAA25k, $M_w = 25000$; PAA250k, $M_w = 250000$) as well as by changing the addition time of the sodium salts of PAA (PAA-Na) to an aqueous solution of calcium carbonate. The precipitation of CaCO_3 was carried out by a double jet method. Stable vaterite crystals were successfully obtained by delaying the addition of all the sodium salts of PAA from 1 to 60 min, and the resulting particles were formed by a spherulitic growth mechanism. The vaterite particles modified with PAA25k-Na and PAA250k-Na showed higher stability than the ones stabilized by PAA1.2k-Na in an aqueous solution. However, in the initial presence of PAA-Na, amorphous calcium carbonate (ACC), vaterite or calcite were induced under various conditions. It is interesting to find that the ACC product induced by PAA1.2k-Na was more stable than that induced by PAA25k-Na in an aqueous solution as well as in a dry state. It was also found that the CaCO_3 particles formed through the nano-aggregation mechanism might be induced by the strong inhibiting effects of PAA-Na, while the spherulitic growth mechanism might be due to the insufficient inhibiting efficiency for the crystallization. These results suggest that the selective interaction of PAA-Na with CaCO_3 at different stages as well as the inhibiting strength varied with the chain lengths of PAA-Na could play an important role for the controlling of the crystal nucleation and growth during the crystallization process.

KEY WORDS: Calcium Carbonate / Mineralization / Calcite / Vaterite / Amorphous Calcium Carbonate / Poly(acrylic acid) / Delayed Addition Method /

The construction of organic—inorganic hybrid materials by biomimetic mineralization under mild conditions have been received much attention in recent years in terms of understanding of the fundamental mechanisms in the biomineralization process as well as developing new materials and new applications.^{1–7} Calcium carbonate (CaCO_3), one of the most abundant inorganic biominerals, exists as three anhydrous crystalline polymorphs (calcite, aragonite, vaterite), two hydrated metastable forms (monohydrocalcite and calcium carbonate hexahydrate), and an unstable amorphous phase.^{8–11}

In biomineralization process, a final crystalline phase might result from a multistage crystallization process, initiated by the formation of an amorphous precursor and crystalline intermediates that undergo subsequent phase transformations.^{4,12–14} The modification of the nucleation and growth of the crystallization process can be controlled by a thermodynamic or kinetic method, and the crystal growth can be mediated by many possible pathways, such as nano-spherulites aggregation-induced crystallization or transformed by a simple crystal growth, and so forth.^{13,15–22} The existence of several phases would enable a living organism to control mineralization through intervention with kinetics. By selectively interacting with the biomineral at different stages during the crystal-forming process, the organism may choose to manipulate both the polymorph and the orientation of the mineral to meet specific biological requirements. Although the presence of various synthetic additives has been extensively studied for biomimetic crystallization,^{23–31} selective interaction of an organic additive with the mineral at different stages of the

crystallization has not been examined in detail.

Recently, we have reported a new concept for controlling crystalline polymorphs of CaCO_3 by the interaction of a synthetic additive at different stages during the crystallization process.^{15,32,33} In our previous work, the sodium salt of poly(acrylic acid) (PAA-Na) (PAA5k, $M_w = 5000$) for selectively interacting with the crystallization of calcium carbonate at different stages was studied by a delayed addition method.³³ Although PAA5k-Na acted as an inhibitor for the crystallization in the initial presence of PAA5k-Na, stable vaterite particles were successfully obtained by delaying the addition of PAA5k-Na from 1 to 60 min. The vaterite particles were stable in an aqueous solution for more than 30 d. We also found a different particle-formation mechanism of the CaCO_3 products. The vaterite particles were formed through the spherulitic growth mechanism by the delayed addition of PAA5k-Na, while a mixture of vaterite and calcite was formed by the nano-aggregation mechanism in the initial presence of PAA5k-Na. Most researches have suggested that vaterite crystal is formed by the aggregation mechanism of nanosized crystallites.^{15–18} However, our findings were the first reports that a stable vaterite particle was formed through a spherulitic growth mechanism by using a simple method modified with a common additive.

In this work, we extended to study the influence of PAA-Na with various molecular weights (PAA1.2k, $M_w = 1200$; PAA25k, $M_w = 25000$; PAA250k, $M_w = 250000$) on the mineralization of CaCO_3 at different stages during the crystal-forming process. Similar to the previous case of PAA5k-Na,

Department of Polymer Chemistry, Graduate School of Engineering, Kyoto University, Katsura, Nishikyo-ku, Kyoto 615-8510, Japan

[†]To whom correspondence should be addressed (Tel: +81-75-383-2609, Fax: +81-75-383-2607, E-mail: ken@chujo.synchem.kyoto-u.ac.jp).

vaterite crystals were obtained by the delayed addition of PAA-Na from 1 to 60 min in all cases of PAA-Na, and the resulting vaterite particles were formed by a spherulitic growth mechanism. Whereas, a variety of phases: amorphous calcium carbonate (ACC), vaterite or calcite products were induced in the cases of the initial presence of PAA-Na under various conditions. We also found that the crystallization mechanisms of CaCO_3 were versatile under different conditions.

EXPERIMENTAL SECTION

Materials

Poly(acrylic acid) (PAA) ($M_w = 5000, 25000$ and 250000), calcium chloride dihydrate and ammonium carbonate were obtained from Wako Pure Chemical Industries, Ltd. PAA ($M_w = 1200$) was purchased from Aldrich. An aqueous solution of PAA-Na was prepared by mixing the same molar ratios of PAA and sodium hydroxide.

Precipitation of CaCO_3

The standard precipitation of CaCO_3 was carried out by a double jet method as follows.³⁴ A 0.1 M CaCl_2 aqueous solution (adjusted to pH 8.5 with dilute aqueous NH_3) and a 0.1 M $(\text{NH}_4)_2\text{CO}_3$ aqueous solution (adjusted to pH 10.0 with aqueous NH_3) were simultaneously injected *via* syringes into distilled water (adjusted to pH 8.5 with dilute aqueous NH_3). An aqueous solution of PAA-Na was then added into the reaction mixture after incubation at 30 °C for several minutes (0, 1, 3, 20, or 60 min). For the addition time of 0 min, the calcium reagents were injected into an aqueous solution containing PAA-Na. This solution was then kept at 30 °C for 1 d with gentle stirring. The concentration of the repeating unit of PAA-Na was constant in all experiments except for those specifically mentioned. The precipitated CaCO_3 product was collected and washed with water for several times and then dried at room temperature under a reduced pressure.

Measurements

The morphologies of CaCO_3 particles were observed by scanning electron microscopy (SEM, JEOL JSM-5600B at 15 kV). The X-ray diffraction (XRD) was analysed on a Rigaku Mini Flex/AW with $\text{CuK}\alpha$ radiation ($\lambda = 1.5406 \text{ \AA}$) in $\theta/2\theta$ mode at room temperature. The 2θ scan data were collected at a 0.01° interval and the scan speed was $1^\circ (2\theta)/\text{min}$. Fourier transform infrared (FT/IR) spectra were recorded with a Perkin-Elmer 2000 spectrometer by a KBr pellet method. Thermogravimetric analysis (TGA) was measured on a TG/DTA 6200 (SEIKO Instruments, Inc.) at a heating rate of $10^\circ\text{C}/\text{min}$ under an air atmosphere.

RESULTS

Effect of the Sodium Salts of Poly(acrylic acid) on the Crystallization of Calcium Carbonate by the Delayed Addition Method

In our previous report, the crystallization of calcium

carbonate by changing the addition time of PAA5k-Na was studied.³³ In this work, we further investigated the influence of the molecular weights of PAA-Na on the crystallization of CaCO_3 by the delayed addition method. The precipitation of CaCO_3 was carried out by the double jet method.³⁴ The two syringe tips were closely joined so that a local high concentration was achieved at the moment when the two reagents (CaCl_2 and $(\text{NH}_4)_2\text{CO}_3$) simultaneously injected into an aqueous solution, which leads to the immediate nucleation of CaCO_3 . After the two reagents were completely injected into the aqueous solution, the aqueous solution of PAA-Na was added into the reaction mixture after incubation at 30 °C for several minutes (1, 3, 20, or 60 min). The experimental conditions and the results are summarized in Table I.

The yields of the obtained precipitates were all about 80% and they showed no remarkable difference for the addition time from 1 to 60 min at the concentration of $[\text{Ca}^{2+}] = [\text{CO}_3^{2-}] = 5.5 \text{ mM}$. This is because the high concentration of calcium reagents exhibits a fast rate of the crystallization, in which the critical point of the sudden increase in the turbidity of the solution was observed before incubation for 1 min.³³

The crystal phase of the obtained products was confirmed by XRD analysis.^{35,36} The XRD patterns exhibit the characteristic reflections of vaterite for all the samples except for the product of run 20 in Table I, in which a mixture of calcite and vaterite was obtained and the fraction of calcite was 14% as identified

Table I. Effect of molecular weights of PAA on the crystallization of CaCO_3 by the delayed addition method^a

run	M_w of PAA	addition time, min	polymorphism ^b	particle size of vaterite, ^c μm	yield, ^d %	adsorbed amount of PAA on particles, ^e %
1	1.2k	0	amorphous	—	11	11.7
2		1	vaterite	3.0 ± 0.9	81	0.9
3		3	vaterite	3.1 ± 0.8	87	1.5
4		20	vaterite	3.1 ± 0.8	82	1.3
5		60	vaterite	3.3 ± 0.8	86	1.2
6 ^f	5k	0	NA	—	0	—
7 ^f		1	vaterite	3.4 ± 1.2	85	1.5
8 ^f		3	vaterite	3.8 ± 1.0	86	1.1
9 ^f		20	vaterite	3.9 ± 0.8	86	1.4
10 ^f		60	vaterite	3.7 ± 0.9	87	1.4
11	25k	0	amorphous	—	39	19.2
12		1	vaterite	3.0 ± 0.7	79	1.4
13		3	vaterite	3.0 ± 0.7	82	1.0
14		20	vaterite	3.0 ± 0.7	83	1.2
15		60	vaterite	3.4 ± 0.9	80	1.3
16	250k	0	vaterite	—	78	10.9
17		1	vaterite	3.4 ± 1.1	78	0.9
18		3	vaterite	3.4 ± 0.9	80	1.3
19		20	vaterite	3.5 ± 0.9	80	1.3
20		60	vaterite + calcite (14%)	3.5 ± 0.9	77	1.0

^aExperimental conditions: $[\text{Ca}^{2+}] = [\text{CO}_3^{2-}] = 5.5 \text{ mM}$, $[-\text{COO}^-]/[\text{Ca}^{2+}] = 0.31$, the pH value of the aqueous solution was adjusted to 8.5 with dilute aqueous NH_3 . ^bPolymorphism was characterized by XRD and FT/IR. ^cThe size of particles was measured by SEM. ^dThe yield was calculated by the final crystal weights compared with the theoretical weights of CaCO_3 from injected calcium reagents. ^eThe adsorbed amount of PAA-Na was measured by TGA (heating rate: $10^\circ\text{C}/\text{min}$ under an air atmosphere). ^fThe data of runs 6 to 10 were obtained from the previous report.³³

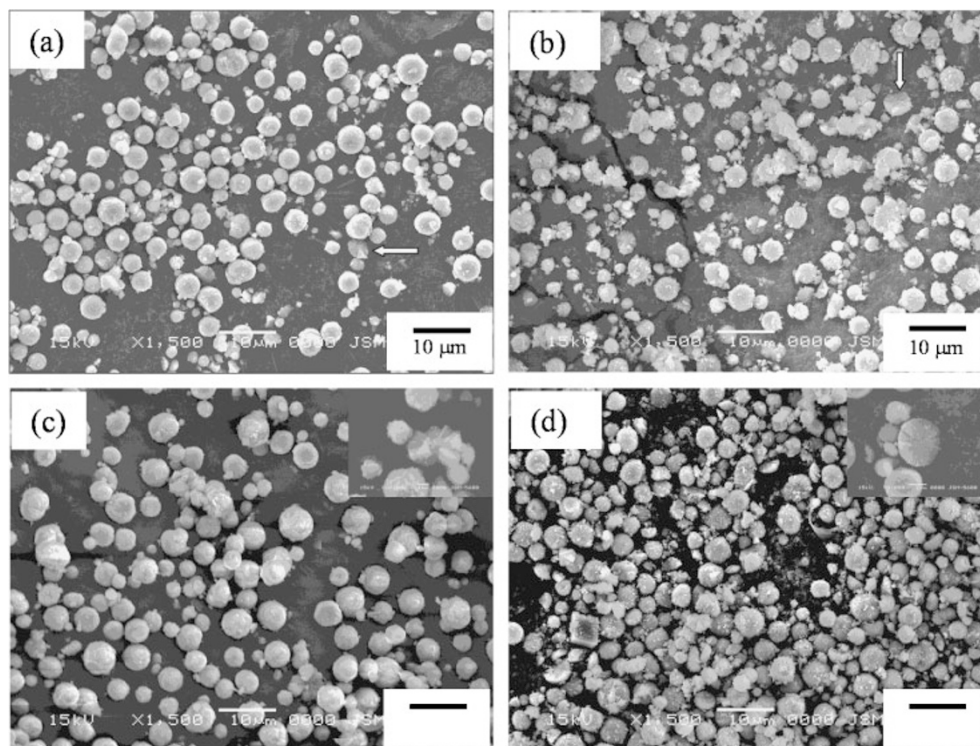


Figure 1. SEM images of the CaCO_3 products of (a) run 2, (b) run 5, (c) run 17 and (d) run 20 in Table I. The arrows show the characteristic radiating features in the crystals. The inset shows the images in the interior of cracked open vaterite particles.

by Rao's equation.³⁷ The crystal phase of the CaCO_3 products was also characterized by FT/IR analysis. All the samples showed two absorption bands at 877 and 746 cm^{-1} , indicating the vaterite polymorph. The product of run 20 showed an additional band at 713 cm^{-1} , which indicates a mixture of calcite and vaterite.^{14,38,39}

The morphologies of the obtained crystals were observed by SEM. Figure 1 shows the typical images of the obtained crystalline products. The average particle sizes of the spherical vaterite particles were around the range of 3 to $4\text{ }\mu\text{m}$ for all the samples. Small fraction of rhombohedral calcite was observed in the product of run 20 (Figure 1d). It was found that the vaterite particles had a spherical shape with smooth surfaces for the early addition time (1 min), whereas the vaterite particles showed a spherical shape with rough surfaces and some irregularly shaped particles for the late addition time (3, 20, and 60 min) in all the cases. In the previous report, we suggested that irregularly shaped particles and rough surfaces in the later addition might be caused by dissolution and recrystallization of the resulting vaterite particles before adding PAA-Na.³³

The amounts of PAA-Na adsorbed on the obtained CaCO_3 crystals were measured by TGA. The adsorbed amount of PAA-Na on the CaCO_3 particles was calculated by the weight loss at $800\text{ }^\circ\text{C}$ after subtracting the weight lost by CaCO_3 .³³ The adsorbed amounts of PAA-Na were in the range of 1 to 1.5 wt% for all the obtained products. We assumed that PAA-Na was mostly adsorbed on the surface of the final vaterite

particles with an average particle size of 3 to $4\text{ }\mu\text{m}$. All the above results demonstrate that the vaterite crystals were stabilized by PAA-Na adsorbed on the surface of the particles.

It is well known that vaterite is the thermodynamically most unstable form of the three crystal phases of CaCO_3 . Without any additives, vaterite phase transforms quickly into stable calcite *via* a solvent-mediated process.^{40,41} We checked the stability of the vaterite products in an aqueous solution for longer incubation of 5 d at $30\text{ }^\circ\text{C}$. Furthermore, in order to check the binding strength between PAA-Na and the surface of the vaterite, the stability of the isolated vaterite particles was also evaluated. The crystal products incubated in the reaction aqueous solution were filtered after 1 d and washed with water, and then the isolated crystals were put into a fresh water for further incubation of 5 d. The results are summarized in Table II.

In the cases of the higher molecular weight, PAA25k-Na and PAA250k-Na, the obtained vaterite products were stable for longer incubation (runs 4 and 6 in Table II). Their isolated vaterite products were also stable for longer incubation under the condition of the earlier addition time (3 min) as well as the higher ratio of $[-\text{COO}^-]/[\text{Ca}^{2+}] = 0.62$ (runs 5 and 7 in Table II). However, in the case of PAA1.2k-Na, the vaterite phase was transformed into calcite for incubation of 5 d in the ratio of $[-\text{COO}^-]/[\text{Ca}^{2+}] = 0.31$ (run 1 in Table II). Under the condition of the higher ratio of $[-\text{COO}^-]/[\text{Ca}^{2+}] = 0.62$, the obtained vaterite product was stable for incubation of 5 d (run 2 in Table II), whereas the isolated vaterite product showed the

Table II. Stability of the vaterite products stabilized by PAA-Na for longer incubation in the aqueous solution^a

run	M_w of PAA	$[\text{Ca}^{2+}]$, mM	$[-\text{COO}^-]/[\text{Ca}^{2+}]$	addition time, min	Polymorphism ^b	yield, ^c %
1	1.2k	5.5	0.31	1	calcite	88
2		2.75	0.62	3	vaterite	46
3 ^d		2.75	0.62	3	calcite	44
4	25k	5.5	0.31	1	vaterite	84
5 ^d		2.75	0.62	3	vaterite	17
6	250k	5.5	0.31	1	vaterite	82
7 ^d		2.75	0.62	3	vaterite	69

^aThe incubation time of the vaterite samples was 5 d in an aqueous solution. ^bPolymorphism was characterized by XRD. ^cThe yield was calculated by the final crystal weights compared with the theoretical weights of CaCO_3 from injected calcium reagents. ^dAfter incubation in the reaction aqueous solution for 1 d, the product was filtered and washed with water, and then incubated in a fresh water for 5 d.

phase transformation into calcite (run 3 in Table II) under the same condition. These results indicate that the vaterite particles modified with the higher molecular weights of PAA-Na exhibited higher stability than those modified with PAA1.2k-Na.

Precipitation of Calcium Carbonate in the Initial Presence of the Sodium Salts of Poly(acrylic acid)

The effect of the initial presence of PAA-Na (addition time = 0 min) with various molecular weights on the mineralization of CaCO_3 was studied. A constant concentration of the calcium reagents ($[\text{Ca}^{2+}] = [\text{CO}_3^{2-}] = 5.5 \text{ mM}$) were injected into an aqueous solution containing PAA-Na with various ratios of $[-\text{COO}^-]/[\text{Ca}^{2+}]$. The results are summarized in Table III. In the previous report, we demonstrated that the initial presence of the medium molecular weight PAA5k-Na acted as a strong inhibitor for the crystal formation when the ratio of $[-\text{COO}^-]/[\text{Ca}^{2+}]$ was higher than 0.1.³³ In the present work, for the lower molecular weight PAA1.2k-Na, ACC was formed in the higher ratio of 0.31 as identified by XRD analysis (Figure 2), in which a relatively low yield of 11% was obtained. When the ratios were lowered to 0.2 and 0.1, calcite crystals were obtained, in which the yields were 16% and 77% corresponding to the ratios of 0.2 and 0.1, respectively. In the case of PAA25k-Na, amorphous product with a low yield of 39% was also formed in the higher ratio of 0.31. While vaterite crystals with yields around 65% were produced in the ratios of 0.2 and 0.1. In the case of PAA250k-Na, vaterite crystals and a small fraction of calcite were formed in the lower ratios of 0.2 and 0.1. The yields of the crystal products were around 80% similar to the results by the delayed addition of PAA-Na. Current results suggest that the mineralization of CaCO_3 could be controlled by the PAA-Na with various chain lengths as well as the ratios of $[-\text{COO}^-]/[\text{Ca}^{2+}]$.

The typical morphological images of the precipitated products were shown in Figure 3. In the case of PAA1.2k-Na, the ACC product (run 1 in Table III) showed irregularly shaped micron-sized particles with some faceted faces (Figure 3a), whereas the obtained calcite products (runs 2 and 3) showed nano-aggregated crystals with irregular shape (Figure 3b). In the case of PAA25k-Na, the amorphous product

Table III. Formation of the precipitation of CaCO_3 mediated in the initial presence of the sodium salts of PAA with various molecular weights^a

run	M_w of PAA	$[-\text{COO}^-]/[\text{Ca}^{2+}]$	polymorphism ^b	yield, ^c %	adsorbed amount of PAA on particles, ^d %
1	1.2k	0.31	amorphous	11	11.7
2		0.2	calcite	16	8.2
3		0.1	calcite	77	3.9
4	25k	0.31	amorphous	39	19.2
5		0.2	vaterite	64	8.8
6		0.1	vaterite	69	5
7	250k	0.31	vaterite	78	10.9
8		0.2	vaterite + calcite (6%)	82	7.6
9		0.1	vaterite + calcite (8%)	83	4.3

^aExperimental conditions: $[\text{Ca}^{2+}] = [\text{CO}_3^{2-}] = 5.5 \text{ mM}$. ^bPolymorphism was characterized by XRD and FT/IR. ^cThe yield was calculated by the final crystal weights compared with the theoretical weights of CaCO_3 from injected calcium reagents. ^dThe adsorbed amount of PAA-Na was measured by TGA (heating rate: $10^\circ\text{C}/\text{min}$ under an air atmosphere).

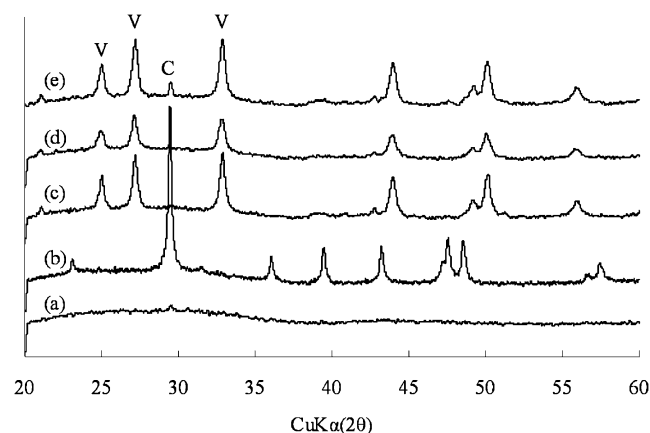


Figure 2. X-Ray diffraction patterns of the products of (a) run 1, (b) run 3, (c) run 6, (d) run 7 and (e) run 9 in Table III. (C: calcite, V: vaterite).

(run 4) and the vaterite product (run 5) obtained in the ratio of 0.2 showed irregularly shaped particles formed from small particles aggregation (Figure 3c). While irregularly shaped particles with rounded surfaces were observed in the obtained vaterite (run 6) in the lower ratio of 0.1 (Figure 3d) as well as the obtained vaterite (run 7) in the case of PAA250k, with higher ratio of 0.31 (Figure 3e). However, the obtained CaCO_3 products showed typically spherical shape of vaterite in the lower ratios of 0.2 and 0.1, (Figure 3f).

The adsorbed amounts of PAA-Na on the CaCO_3 particles increased upon increasing the ratio of $[-\text{COO}^-]/[\text{Ca}^{2+}]$. The adsorbed contents of PAA-Na were in the range from 4 wt % ($[-\text{COO}^-]/[\text{Ca}^{2+}] = 0.1$) to 11–19 wt % ($[-\text{COO}^-]/[\text{Ca}^{2+}] = 0.31$). To compared with the amounts of PAA-Na (1 to 1.5 wt %) adsorbed on the vaterite particles formed by the delayed addition, the present results indicate that the adsorbed PAA-Na were not only adsorbed on the surface of the CaCO_3 particles, but also incorporated inner the particles.

ACC is the least stable phase of CaCO_3 and transforms rapidly into one of the crystalline polymorphs unless it is stabilized by specific additives.⁴² Long-term stability of the

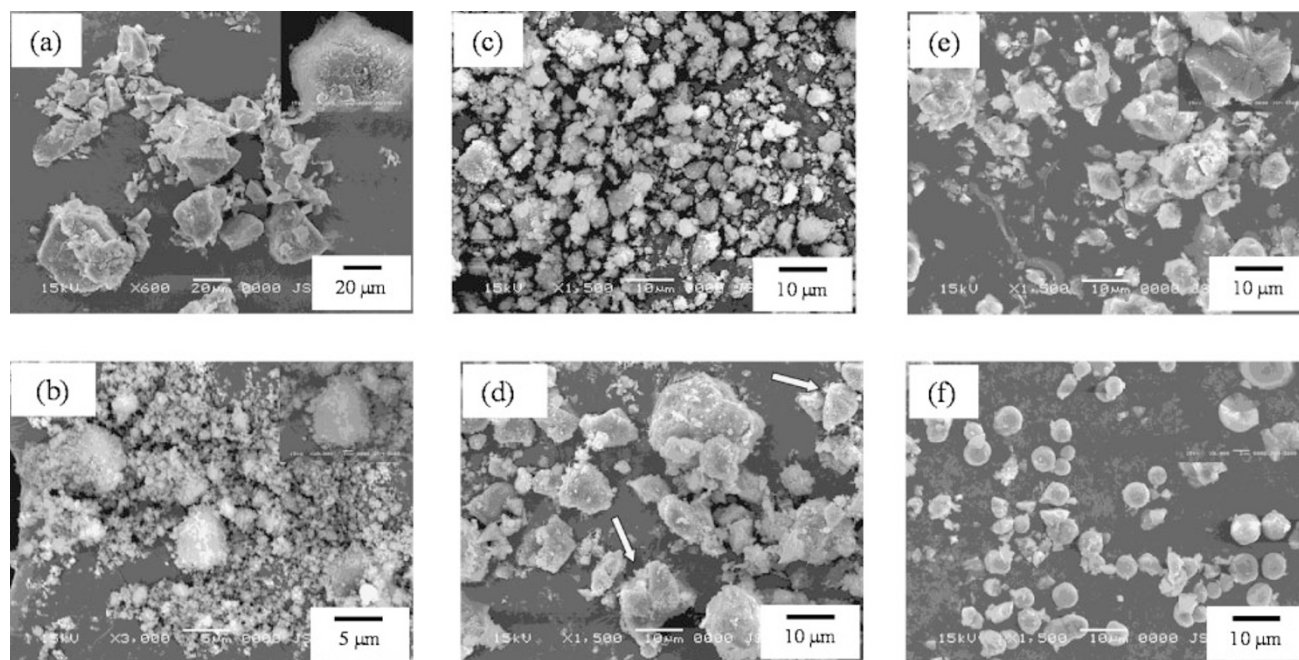


Figure 3. SEM images of the CaCO_3 products of (a) run 1, (b) run 3, (c) run 4, (d) run 6, (e) run 7 and (f) run 9 in Table III. The arrows show the characteristic radiating features in the crystals. The inset shows the enlarged images of cracked open CaCO_3 particles.

ACC products induced by PAA1.2k-Na and PAA25k-Na was studied in an aqueous solution and in a dry state. The results are summarized in Table IV.

The ACC stabilized by PAA1.2k-Na was stable for 3 d (run 2 in Table IV) in an aqueous solution with gentle stirring, while a fraction of ACC transformed into calcite after incubation of 5 d as identified by FT/IR^{42,43} (run 3 in Table IV, and Figure 4b). Furthermore, the ACC was stable for more than 16 months in a dry state (Figure 4c). The ACC stabilized by PAA25k-Na was stable for 1 d, while transformed into a crystalline mixture of vaterite and calcite after incubation of 2 d in an aqueous solution even increased the ratio of $[-\text{COO}^-]/[\text{Ca}^{2+}]$ to 0.4 (run 9 in Table IV). In the dry state, the modified ACC was stable for 6 months, but transformed into a mixture of ACC and calcite after 1 year (Figure 4d). The results suggest that PAA1.2k-Na acts as a stronger stabilizer of ACC than PAA25k-Na does.

DISCUSSION

In this report, vaterite particles were formed by delaying addition of PAA-Na, except the case of PAA250k-Na in the late addition time of 60 min (run 20 in Table I), in which a mixture of vaterite and calcite was formed. A lower efficiency of the interaction between the long chained PAA-Na and Ca^{2+} may be caused by the fact that the long chained polyelectrolyte exhibits a lower mobility in water and has a smaller numbers of the polyelectrolyte chains in the same concentration of repeating units. We assume that some vaterite crystals might phase transform into calcite through the dissolution and recrystallization process with longer incubation time (60 min),

Table IV. Long-term stability of the obtained ACC^a

run	M_w of PAA	$[-\text{COO}^-]/[\text{Ca}^{2+}]$	incubation time, day	Polymorphism ^b	yield, ^c %
1	1.2k	0.31	1	amorphous	11
2		0.31	3	amorphous	15
3		0.31	5	amorphous + calcite	12
4 ^d		0.31	16 months	amorphous	—
5	25k	0.31	1	amorphous	39
6 ^d		0.31	6 months	amorphous	—
7 ^d		0.31	12 months	amorphous + calcite	—
8		0.4	1	amorphous	50
9		0.4	2	vaterite + calcite	64
10		0.4	3	vaterite + calcite	62

^aExperimental conditions: $[\text{Ca}^{2+}] = [\text{CO}_3^{2-}] = 5.5 \text{ mM}$. ^bPolymorphism was characterized by XRD and FT/IR. ^cThe yield was calculated by the final crystal weights compared with the theoretical weights of CaCO_3 from injected calcium reagents. ^dThe CaCO_3 samples were kept at room temperature under dry conditions.

because the long chained PAA-Na might not effectively stabilize the increasing amount of the smaller recrystallization particles to prevent the phase transformation.

The phase transformation of vaterite to the thermodynamically most stable calcite usually occurs easily and irreversibly within 3 d when vaterite particles are in contact with water.^{15,32,44} It was found that the stabilizing ability of the vaterite products modified by the higher molecular weights of PAA-Na was stronger than that by PAA1.2k-Na. In the previous report, we proposed that the strong stabilizing effect was attributed to the strong binding strength between PAA-Na

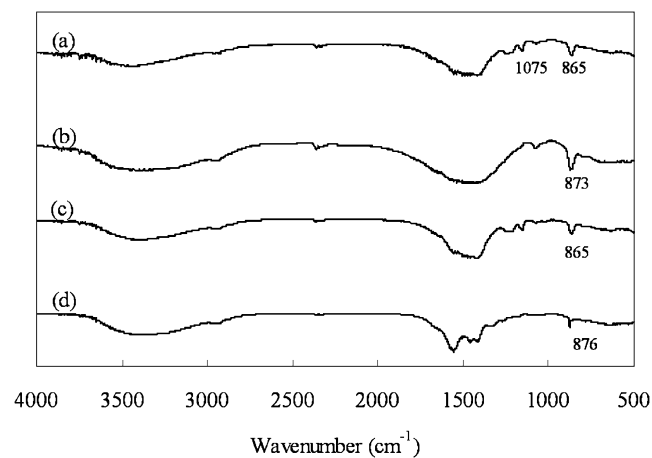


Figure 4. FT/IR spectra of the products of (a) run 1, (b) run 3, (c) run 4, and (d) run 7 in Table IV.

and the surfaces of the vaterite particles.³³ Fantinel *et al.* reported that the binding strength between PAA-Na and Ca^{2+} is stronger with increasing the molecular weights, due to the increased torsion and the bichelating mechanism in the longer polyelectrolyte chains.⁴⁵ Therefore, PAA1.2k-Na may exhibit weaker binding strength on the surfaces of the vaterite particles than the higher molecular weights of PAA-Na. Furthermore, the shorter chained polyelectrolyte might be reversibly attached and desorbed on the crystal surface due to their higher mobility in water.⁴⁶ Therefore, the vaterite particles modified with PAA1.2k-Na was easier to phase transform into calcite due to the easier desorption of the polyelectrolyte for the longer incubation.

In the case of the initial presence of PAA-Na, it is interesting to find that different CaCO_3 phases were induced with the various inhibiting ability of PAA-Na. Imai *et al.* reported that PAA behaves as a suppressant and template for the crystallization of the calcite crystal. The inhibition strength of PAA increased with an increase of the molecular weights of PAA according to the decrease of the grain sizes of calcite.⁴⁶ Interestingly, this is an opposite result with our work which evidently is due to the differing conditions of the crystallization of CaCO_3 . To compare with our previous report, PAA5k-Na acted as a strong inhibitor for the nucleation and growth of the crystallization.³³ The behavior of the inhibition strength of PAA-Na should play an important factor affecting the mineralization of CaCO_3 . For the lower molecular weight of PAA-Na, the higher mobility of PAA-Na in water may cause faster adsorption on the nuclei precursors to inhibit crystal growth. Furthermore, the numbers of the polyelectrolyte chains may also affect the binding efficiency between $-\text{COO}^-$ and Ca^{2+} . Therefore, the ACC products were stabilized by PAA1.2k-Na and PAA25k-Na with stronger inhibiting behavior in the higher ratio of $[-\text{COO}^-]/[\text{Ca}^{2+}] = 0.31$, but the amorphous phase can not be stabilized by PAA250k-Na under the same condition. It should be noted that the moderate chain length of PAA5k-Na showed the strongest inhibiting ability to prevent the formation of crystals.³³ Higher stability of ACC has

been reported to be related with higher disordered structures of the intermediate range ordering.^{42,43,47} The ACC product stabilized by PAA1.2k-Na has higher stability than that induced by PAA25k-Na. The ACC induced by PAA1.2k-Na might exhibit a more disordered structure of intermediate range ordering than the one stabilized by PAA25k-Na. There are two possible reasons. First, PAA1.2k-Na is a stronger inhibitor than PAA25k-Na on the nucleation and crystal growth of CaCO_3 .⁴³ Furthermore, in the Fantinel's report,⁴⁵ PAA1.2k-Na shows slower reaction kinetics of PAA- Ca^{2+} complexation transforming from transient intermediates to a final chelating bidentate complex, in which a more randomly PAA- Ca^{2+} coordination might be induced.⁴³ Therefore, higher stability of ACC was induced by PAA1.2k-Na than by PAA25k-Na.

When the inhibiting strength decreased with decreasing the ratio of $[-\text{COO}^-]/[\text{Ca}^{2+}]$, calcite and vaterite were induced by PAA1.2k-Na and PAA25k-Na, respectively. The calcite induced by PAA1.2k-Na may be explained by the fact that selective adsorption onto the specific crystal faces is favored by the shorter chain.³¹ Therefore, the conformation of the shorter chain of PAA1.2k-Na, which basically fits the (104) and (001) planes of calcite, may selectively adsorb on these planes and suppress the crystal growth.⁴⁶ While, the polycrystalline vaterite exhibiting spherical shaped particles were formed due to the non-selective adsorption of the long chained PAA-Na on the surfaces of CaCO_3 crystals.^{20,31} Furthermore, it was reported that the formation of vaterite was favored under the condition of high pH environment ($\text{pH} = 10$) at room temperature.^{32,48}

In this work, we found that different CaCO_3 particles-formation mechanisms were formed. All the vaterite products in Table I obtained by the delayed addition of PAA-Na were observed exhibiting the characteristic radiating features, which indicate a spherulitic growth mechanism, as shown in the images of insect and as the arrow indicating in Figure 1. In our previous report, we assumed that the initially formed amorphous precursors might grow and transform to larger vaterite particles before the addition of PAA-Na by the double jet method.³³ In the double jet method,³⁴ the nucleation occurred immediately when the calcium reagents injected simultaneously into an aqueous solution and then immediately transported to regions of a lower CaCO_3 concentration for further growing. Before the addition of PAA-Na, the initially formed amorphous precursors may further grow by the dissolution of other ACC nuclei and transform to larger vaterite particles with decreasing amounts of particles. Such larger particles might be difficult to aggregate as a result of the lower surface energy compared with the higher surface energy of nanosized crystallites. Furthermore, a limited numbers of the nanosized crystallites were formed as a heterogeneous nucleation mechanism which may also be difficult to aggregate due to insufficient amounts of nanocrystallites.

However, in the initial presence of PAA-Na, both spherulitic growth and nano-aggregation mechanisms were found under different conditions. Under the conditions of the shorter chain lengths or the higher ratios of $[-\text{COO}^-]/[\text{Ca}^{2+}]$, nanosized

amorphous nuclei might be preformed in the aqueous solution, and they were stabilized with the stronger inhibitor PAA-Na to inhibit the nucleation of crystalline products as a literature reported.⁴⁹ Therefore, the final ACC particles were formed by the aggregation of nanosized ACC precursors. The amorphous precursors would transform to vaterite or calcite nanocrystallites with decreasing inhibiting efficiency of PAA-Na in the lower ratios of $[-\text{COO}^-]/[\text{Ca}^{2+}]$, and the final crystal particles were also formed by the aggregation of nanocrystallites. While under the conditions of PAA250k-Na or PAA25k-Na in the lower ratio of $[-\text{COO}^-]/[\text{Ca}^{2+}] = 0.1$, the SEM images of the interior of cracked crystal particles show that the resulted crystals were formed by the spherulitic growth mechanism (Figure 3d–3f). The initially formed amorphous precursors in the aqueous solution containing the longer chains of PAA-Na might transform and grow to larger crystallites, which is similar to the environment in an aqueous solution before the addition of PAA-Na or the condition of the initial presence of PAA5k-Na when the ratio of $[-\text{COO}^-]/[\text{Ca}^{2+}]$ was 0.01 in the previous report.³³ This indicates that the longer chained PAA-Na has no effectively inhibiting efficiency on the crystal nucleation and growth, which may be caused by the lower mobility in water, a smaller amount of the polyelectrolyte chains in the case of PAA250k-Na or insufficient content of PAA25k-Na in the ratio of $[-\text{COO}^-]/[\text{Ca}^{2+}] = 0.1$.

It is also interesting to find that the adsorbed amounts of PAA-Na on the CaCO_3 particles formed in the initial presence of PAA-Na were higher than those in the delayed addition at the same calcium concentration of 5.5 mM. Under the conditions of the shorter chain lengths or the higher ratios of $[-\text{COO}^-]/[\text{Ca}^{2+}]$, the higher adsorbed amounts of PAA-Na were caused by the adsorption on the surface of the nanoparticles, followed by the nano-aggregation mechanism. However, the higher adsorbed amounts of PAA-Na were also achieved by the spherulitic growth in the initial presence of PAA-Na. It indicates that the adsorbed PAA-Na were not only adsorbed on the surface of the CaCO_3 particles, but also incorporated inner the particles. Therefore, it also means that the adsorption of the longer chain of PAA-Na on the surface of the CaCO_3 particles may not inhibit the crystal growth.

A summary from the CaCO_3 particles-formation mechanism with various chain lengths of the polyelectrolyte PAA-Na is proposed in Scheme 1. By the delayed addition of PAA-Na, stable vaterite crystals were formed by the spherulitic growth mechanism, which showed a characteristic radiating feature in the interior of the cracked vaterite particle. The adsorbed amounts of PAA-Na in the range of 1 to 1.5 wt% on the vaterite particles demonstrate that PAA-Na was mostly adsorbed on the surface of the final particles with an average particle size of 3 to 4 μm .

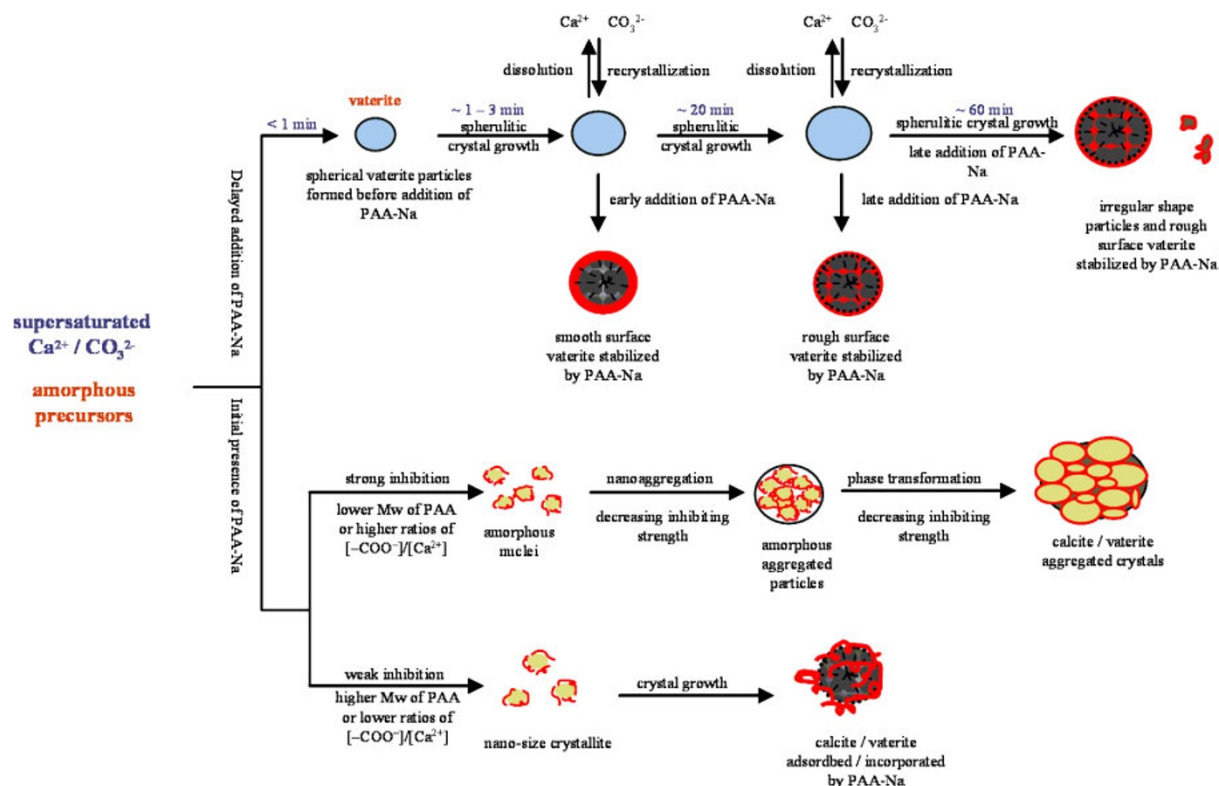
Under the conditions of the initial presence of PAA-Na, the behavior of the inhibiting effect acts as a major factor for controlling the mineralization of CaCO_3 . The combined effects of mobility in water, numbers of polyelectrolyte chains, and binding strength of PAA-Ca^{2+} , which are affected by the chain lengths of PAA-Na, were proposed to exhibit variable inhibit-

ing strength on the nucleation and crystal growth. Under the conditions of the shorter chain lengths or the higher ratios of $[-\text{COO}^-]/[\text{Ca}^{2+}]$, the stronger inhibiting efficiency of PAA-Na adsorbed on the nanosized amorphous precursors to prevent crystal nucleation and growth. Nanosized amorphous nuclei, nano-aggregated ACC particles, and nano-aggregated vaterite or calcite particles were formed through the nano-aggregation mechanism with gradually decreasing the inhibiting strength of PAA-Na. When the inhibiting strength becomes much weaker under the conditions of the longer chain lengths or the lower ratios of $[-\text{COO}^-]/[\text{Ca}^{2+}]$, the amorphous precursors might transform and grow to the larger crystallites due to insufficient inhibiting efficiency on the crystal nucleation and growth. Thus, the crystal particles were formed by the spherulitic growth mechanism. From the present results, we should emphasize that this finding is the first report of the particle-forming mechanisms of CaCO_3 varied with the variable inhibiting strength by using a common polyelectrolyte additive as well as by changing the addition time of polymer additives.

CONCLUSIONS

We studied the mineralization of CaCO_3 by using a common polyelectrolyte additive PAA-Na. We found that the crystallization mechanisms of CaCO_3 can be controlled by the molecular weights of PAA-Na as well as by the addition time of PAA-Na. The present results show that stable vaterite particles were successfully obtained by delaying the addition of PAA-Na from 1 to 60 min, in which PAA-Na was adsorbed on the surface of the vaterite particles to stabilize the unstable phase, and the resulting vaterite particles were formed by the spherulitic growth mechanism. The vaterite particles modified with PAA25k-Na and PAA250k-Na were stable for 5 d in the aqueous solution. While the vaterite particles modified with PAA1.2k-Na transformed into more stable calcite for longer incubation, which may be caused by the weaker binding strength of PAA-Ca^{2+} , and higher mobility in water.

In the case of the initial presence of PAA-Na, PAA-Na with various chain lengths exhibit the variable inhibiting effects on the nucleation and crystal growth. Under the conditions of the shorter chain lengths or the higher ratios of $[-\text{COO}^-]/[\text{Ca}^{2+}]$, amorphous nuclei, nano-aggregated ACC, and nano-aggregated vaterite or calcite particles were induced through the nano-aggregation mechanism, which was controlled by the strong inhibiting effects of PAA-Na. Interestingly, the ACC particles induced by PAA1.2k-Na exhibited higher stability than that formed by PAA25k-Na in an aqueous solution and in a dry state. While under the conditions of the longer chain lengths or the lower ratios of $[-\text{COO}^-]/[\text{Ca}^{2+}]$, the vaterite or calcite crystals were formed by the spherulitic growth mechanism due to insufficient inhibiting efficiency. From the present results, we suggest that the variable inhibiting ability of PAA-Na by varying the chain lengths and the selective interaction of PAA-Na with CaCO_3 at different stages can provide a simple method for the controlling of the crystal nucleation and growth. The



Scheme 1. Schematic Depiction of the Formation of CaCO_3 Spherulites and the Transformation from the Amorphous Phase to Vaterite and Calcite Crystals.

specific interactions of PAA-Na and Ca^{2+} ions play an important role for the mediation of the crystal nucleation and growth during the crystallization process.

Received: October 5, 2007

Accepted: November 7, 2007

Published: December 18, 2007

REFERENCES

- S. Mann, "Biomineralization: Principles and Concepts in Bioinorganic Material Chemistry," Oxford University Press, New York, 2001.
- E. Bauerlein, "Biomineralization: Progress in Biology, Molecular Biology and Application," Wiley-VCH, Weinheim, Germany, 2004.
- K. Gorna, R. Muñoz-Espí, F. Gröhn, and G. Wegner, *Macromol. Biosci.*, **7**, 163 (2007).
- Z. Tang, N. A. Kotov, S. Magonov, and B. Ozturk, *Nat. Mater.*, **2**, 413 (2003).
- L. Addadi and S. Weiner, *Nature*, **389**, 912 (1997).
- B. L. Smith, *Nature*, **399**, 761 (1999).
- S. Mann and G. A. Ozin, *Nature*, **382**, 313 (1996).
- J. Küther, R. Seshadri, W. Knoll, and W. Tremel, *J. Mater. Chem.*, **8**, 641 (1998).
- H. Wei, Q. Shen, Y. Zhao, D.-J. Wang, and D.-F. Xu, *J. Cryst. Growth*, **250**, 516 (2003).
- X. Xu, J. T. Han, and K. Cho, *Chem. Mater.*, **16**, 1740 (2004).
- J. T. Han, X. Xu, D. H. Kim, and K. Cho, *Chem. Mater.*, **17**, 136 (2005).
- J. Perić, M. Vučak, R. Krstulović, L. Brečević, and D. Kralj, *Thermochimica Acta*, **277**, 175 (1996).
- H. Cölfen and S. Mann, *Angew. Chem., Int. Ed.*, **42**, 2350 (2003).
- G. Xu, N. Yao, I. A. Akasay, and J. T. Groves, *J. Am. Chem. Soc.*, **120**, 11977 (1998).
- D.-K. Keum, K. Naka, and Y. Chujo, *Bull. Chem. Soc. Jpn.*, **76**, 1687 (2003).
- H. Cölfen and M. Antonietti, *Langmuir*, **14**, 582 (1998).
- L. Brečević, V. Nöthig-Laslo, D. Kralj, and S. Popović, *J. Chem. Soc., Faraday Trans.*, **92**, 1017 (1996).
- Z. Zhang, D. Gao, H. Zhao, C. Xie, G. Guan, D. Wang, and S.-H. Yu, *J. Phys. Chem. B*, **110**, 8613 (2006).
- N. Goldenfeld, *J. Cryst. Growth*, **84**, 601 (1987).
- J.-P. Andreassen, *J. Cryst. Growth*, **274**, 256 (2005).
- A.-X. Xu, Y. Ma, and H. Cölfen, *J. Mater. Chem.*, **17**, 415 (2007).
- H. Cölfen and S. Mann, *Angew. Chem., Int. Ed.*, **44**, 5576 (2005).
- K. Naka and Y. Chujo, *Chem. Mater.*, **13**, 3245 (2001).
- T. Kato, A. Sugawara, and N. Hosoda, *Adv. Mater.*, **14**, 869 (2002).
- H. Cölfen, *Curr. Opin. Colloid Interface Sci.*, **8**, 23 (2003).
- H. Cölfen and L. Qi, *Chem. Eur. J.*, **7**, 106 (2001).
- N. Ueyama, T. Hosoi, Y. Yamada, M. Doi, T. Okamura, and A. Nakamura, *Macromolecules*, **31**, 7119 (1998).
- F. Manoli and E. Dalas, *J. Cryst. Growth*, **222**, 293 (2001).
- T. Kato, T. Suzuki, T. Amamiya, T. Irie, M. Komiyama, and H. Yui, *Supramol. Sci.*, **5**, 411 (1998).
- L. A. Gower and D. A. Tirrell, *J. Cryst. Growth*, **191**, 153 (1998).
- S.-H. Yu and H. Cölfen, *J. Mater. Chem.*, **14**, 2124 (2004).
- K. Naka, D.-K. Keum, Y. Tanaka, and Y. Chujo, *Bull. Chem. Soc. Jpn.*, **77**, 827 (2004).
- K. Naka, S.-C. Huang, and Y. Chujo, *Langmuir*, **22**, 7760 (2006).
- M. Sedlák, M. Antonietti, and H. Cölfen, *Macromol. Chem. Phys.*, **199**, 247 (1998).
- Joint Committee on Powder Diffraction Standards—International Center for Diffraction Data, file no. 13-192 (Vaterite).
- Joint Committee on Powder Diffraction Standards—International Center for Diffraction Data, file no. 47-1743 (Calcite).
- M. S. Rao, *Bull. Chem. Soc. Jpn.*, **46**, 1414 (1973).

38. D. Chakrabarty and S. Mahapatra, *J. Mater. Chem.*, **9**, 2953 (1999).
39. L. Wang, I. Sondi, and E. Matijević, *J. Colloid Interface Sci.*, **218**, 545 (1999).
40. A. López-Macipe, J. Gómez-Morales, and R. Rodríguez-Clemente, *J. Cryst. Growth*, **166**, 1015 (1996).
41. D. Kralj, L. Brečević, and J. Kontrec, *J. Cryst. Growth*, **177**, 248 (1997).
42. L. Addadi, S. Raz, and S. Weiner, *Adv. Mater.*, **15**, 959 (2003).
43. S.-C. Huang, K. Naka, and Y. Chujo, *Langmuir*, in press (2007).
44. K. Naka, Y. Tanaka, and Y. Chujo, *Langmuir*, **18**, 3655 (2002).
45. F. Fantinel, J. Rieger, F. Molnar, and P. Hübler, *Langmuir*, **20**, 2539 (2004).
46. A. Kotachi, T. Miura, and H. Imai, *Chem. Mater.*, **16**, 3191 (2004).
47. N. Koga, Y. Nakagoe, and H. Tanaka, *Thermochim. Acta*, **318**, 239 (1998).
48. N. Spanos and P. G. Koutsoukos, *J. Phys. Chem. B*, **102**, 6679 (1998).
49. M. Balz, H. A. Therese, J. Li, J. S. Gutmann, M. Kappl, L. Nasdala, W. Hofmeister, H.-J. Butt, and W. Tremel, *Adv. Funct. Mater.*, **15**, 683 (2005).